# UNITED STATES
# NAVAL POSTGRADUATE SCHOOL

## DEPARTMENT OF AERONAUTICS

## TECHNICAL NOTE
## NO. 65-3

A GRAPHICAL SOLUTION OF THE MATCHING PROBLEM
IN CLOSED-CYCLE GAS TURBINE PLANTS

by

M. H. VAVRA

Aero Dept.

1 9 6 5

TN NO.

UNITED STATES NAVAL POSTGRADUATE SCHOOL
DEPARTMENT OF AERONAUTICS
PROPULSION LABORATORIES
TECHNICAL NOTE
NO.

# A GRAPHICAL SOLUTION OF THE MATCHING PROBLEM IN CLOSED-CYCLE GAS TURBINE PLANTS

M. H. Vavra

ABSTRACT

The paper describes a graphical method for the solution of the matching problem in gas turbine plants. The method is used to investigate the conditions in a closed-cycle system similar to that of the ML-1 nuclear gas turbine plant of Aerojet-General Nucleonics. It is shown that proper matching of the turbomachines with a given system is of great importance to obtain the best possible performance.

## NOMENCLATURE

| | |
|---|---|
| $k$ | constant for pressure drop calculations |
| $\dot{m}$ | mass flow rate (lbm/sec) |
| $p$ | total pressure (psia) |
| $p_{ATM}$ = | 760 mm Hg = 14.7 psia |
| $r$ | pressure ratio |
| $N$ | speed (rpm) |
| KW | power (KW) |
| $T$ | total absolute temperature |
| $T_{ATM}$ = | 288°K = 518.4° R |
| $V$ | velocity |
| $\delta$ = | $p/p_{ATM}$ |
| $\theta$ = | $T/T_{ATM}$ |
| $\mu$ | leakage flow coefficient |
| $\xi$ | pressure drop coefficient |
| $\rho$ | mass density of fluid |

Subscripts

| | |
|---|---|
| 1 | refers to compressor inlet |
| 2 | " " compressor discharge |
| 3 | " " turbine inlet |
| 4 | " " turbine discharge |
| C | " " compressor |
| T | " " turbine |
| S | " " shaft power |
| HP | " " high pressure side of loop |
| LP | " " low pressure side of loop |

CAPTIONS FOR FIGURES

## INTRODUCTION

In closed-cycle gas turbine plants it is quite difficult to evaluate the influence of the different components on the performance of the whole system. These difficulties arise because of the shifting of the operating points of the turbomachines, that produces changes in pressure ratios and mass flow rates. Without a computer it is necessary to perform lengthy calculations with methods of successive approximations to determine these changes. Even if a computer program is available the graphical method for the solving of the matching problem, which is discussed in the following, has merits since it gives a good insight how the performance of the different components affect the operating conditions of the plant.

The method will be applied to the simple cycle of the nuclear ML-1 plant of Aerojet-General Nucleonics of Fig. 1. It is assumed that the performance maps of the turbomachines are given, that the pressure drops in the system be known, and that the plant operates between given temperature levels. More complicated cycles with multiple compressors and turbines, having intercooling and reheat, can be investigated with the same general principles that are outlined in this paper.

If $\dot{m}_C$ denotes the mass flow rate entering the compressor of Fig. 1, the turbine flow rate $\dot{m}_T$ is

$$\dot{m}_T = (1 - \mu)\, \dot{m}_C \qquad \text{(lbm/sec)} \tag{1}$$

where $\mu$ represents that fraction of the flow rate which escapes from the high pressure to the low pressure side of the loop, either through the bypass control valve, or through seals and leakage paths. The fluid that escapes from the loop to the surroundings is replenished by a make-up system, controlled by the pressure of the cycle. The power required for the compression of the make-up gas will be ignored.

The pressure $p_3$ ahead of the turbine can be expressed by

$$p_3 = (1 - \xi_{HP})\, p_2 \tag{2}$$

where $p_2$ is the compressor discharge pressure and $\xi_{HP}$ a factor that depends on the pressure drops in the whole high pressure loop.

The turbine discharge pressure $p_4$ can be expressed similarly by

$$p_4 = (1 + \xi_{LP})\, p_1 \tag{3}$$

with the compressor inlet pressure $p_1$, and the pressure loss coefficient $\xi_{LP}$ of the low pressure loop of the plant. The pressure ratio $r_T = p_3/p_4$ of the turbine is then related to the pressure ratio $r_C = p_2/p_1$ of the compressor by

$$r_T = \frac{(1 - \xi_{HP})}{(1 + \xi_{LP})} r_C \tag{4}$$

Since the turbomachines of the plant under discussion are directly coupled, compressor speed $N_C$ must equal the turbine speed $N_T$. This condition, and Eqs. 1 to 4, must be satisfied, and made compatible with the performance of the turbomachines, as given by their maps, to solve the matching problem of the system.

The performance of a compressor that operates with a particular fluid can be represented by

$$r_C = \frac{p_2}{p_1} = f_1\left(\frac{\dot{m}_C \sqrt{\theta_1}}{\delta_2}, \frac{N_C}{\sqrt{\theta_1}}\right) \tag{5}$$

and

$$\frac{KW_C}{\delta_1 \sqrt{\theta_1}} = f_2\left(\frac{\dot{m}_C \sqrt{\theta_1}}{\delta_2}, \frac{N_C}{\sqrt{\theta_1}}\right) \tag{6}$$

where $KW_C$ represents the power in KW to drive the machine. The quantities $\theta$ and $\delta$ are defined by

$$\theta = T/T_{ATM}$$

$$\delta = p/p_{ATM}$$

The arbitrarily chosen reference values $T_{ATM} = 288^{o}K = 518.4^{o}$ R, and $p_{ATM} = 760$ mm Hg $= 14.7$ psia, make it possible to express the referred flow rates, speeds, and power requirements with conventional units. The subscripts of $\theta$ and $\delta$ correspond to the stations in Fig. 1 where the total absolute temperatures T and the total absolute pressures p occur.

In contrast to usual practice the referred flow rate of the compressor is taken with respect to the <u>discharge</u> pressure and the <u>inlet</u> temperature, for convenience in the later calculations. If the flow rate $\dot{m}_C \sqrt{\theta_1}\delta_1$ is given instead of the quantity used in Eqs. 5 and 6, the latter can be established also, since at a particular referred speed $N_C/\sqrt{\theta_1}$ and a referred flow rate $\dot{m}_C\sqrt{\theta_1}/\delta_1$ there occurs only one pressure ratio $p_2/p_1$. Then

$$\frac{\dot{m}_C \sqrt{\theta_1}}{\delta_2} = \frac{\dot{m}_C \sqrt{\theta_1}}{\delta_1} \frac{p_1}{p_2}$$

It is of interest to note that the referred power of Eq. 6 is the power necessary to drive a compressor whose inlet conditions correspond to the standard atmosphere defined above, and whose speed is such that the same velocity triangles occur as in the actual machine.

For the present study it is advantageous to express the performance of a turbine by

$$\frac{\dot{m}_T \sqrt{\theta_3}}{\delta_3} = f_3\left(\frac{p_3}{p_4}, \frac{N_T}{\sqrt{\theta_3}}\right) \tag{7}$$

and

$$\frac{KW_T}{\delta_3 \sqrt{\theta_3}} = \left(\frac{p_3}{p_4}, \frac{N_T}{\sqrt{\theta_3}}\right) \tag{8}$$

The referred turbine flow rate of Eq. 7 and the referred shaft power of Eq. 9 represent the flow rate and power, respectively, that the turbine would have if the inlet conditions of the gas were those of the standard atmosphere.

Two turbocompressor sets were developed for the ML-1 plant. One, which henceforth will be called TC-set "a", has a two-stage centrifugal compressor and a two-stage axial turbine, operating at a nominal speed of about 18,000 rpm at 118°F = 48°C compressor inlet temperature, and 1200°F = 650°C turbine inlet temperature. The other set ("B") has an eleven-stage axial compressor and a two-stage axial turbine with a design speed of about 22,000 rpm at the above-listed temperatures. Both sets operate with nitrogen as working fluid, to which 5% oxygen is added to prevent nitriding of the reactor materials.

Although the method of this paper can be used to obtain matching solutions at arbitary speeds and cycle temperatures, the present investigations will be restricted to the above-mentioned temperature levels and the design speeds of the TC sets. Then, for TC set "A":

$$\frac{N_C}{\sqrt{\theta_1}} = 17{,}170 \text{ rpm, and, } \frac{N_T}{\sqrt{\theta_3}} = 10{,}130 \text{ rpm}$$

For TC set "B":

$$\frac{N_C}{\sqrt{\theta_1}} = 20{,}620 \text{ rpm, and, } \frac{N_T}{\sqrt{\theta_3}} = 12{,}160 \text{ rpm}$$

For these referred speeds the functions $f_1$ of Eq. 5 of the compressors of both TC sets are presented in Fig. 2. The functions $f_3$ of Eq. 7 for the turbines are shown in Fig. 3. It can be noted that both figures have the same double logarithmic scales since this representation is required for the present method. Fig. 4 and 5 give the powers required by the compressors, and produced by the turbines, respectively, at the referred

design speeds, in accordance with Eqs. 6 and 8. The data in Figs. 2 and 5 pertain to the state of the TC sets as they were initially designed and fabricated, and represent the best estimate of their initial performance obtained by a number of tests with different instrumentation at various conditions.

## SYSTEM PRESSURE LOSSES

Pressure drops due to friction, flow separations, or mixing can be expressed by

$$\Delta p = f \rho V^2$$

where the dimensionless coefficient $f$ may vary with Reynolds number. The quantities $\rho$ and $V$ are the average mass density of the fluid and the average flow velocity in the element where the total pressure is reduced by $\Delta p$. Since $V = \dot{m}/(\rho A)$, where A is the cross-sectional flow area, there is with $\rho \propto p/T$,

$$\frac{\Delta p}{p} = c \frac{\dot{m}^2 T}{p^2} \tag{10}$$

The quantity $c$ is a constant for a particular element of a system. The total pressure drop in the low pressure side of the loop of Fig. 1 may be expressed by using Eqs. 3 and 10

$$\frac{p_4 - p_1}{p_1} = \xi_{LP} = \sum c_i \frac{\dot{m}^2 T_i}{p_i^2}$$

where the index i refers to the different elements that produce pressure drops. For small values of $\xi_{LP}$ there is $p_i \approx p_1$, and with $\dot{m} = \dot{m}_C$

$$\xi_{LP} = \left(\frac{\dot{m}_C \sqrt{\theta_1}}{\delta_2}\right)^2 \left(\frac{p_2}{p_1}\right)^2 \sum \left(c_i \frac{T_i}{T_1} \frac{T_{ATM}}{p_{ATM}}\right) \tag{11}$$

If the temperatures in the loop remain nearly constant, Eq. 11 may be written as

$$\xi_{LP} = k_{LP} \left(\frac{\dot{m}_C \sqrt{\theta_1}}{\delta_2}\right)^2 \left(\frac{p_2}{p_1}\right)^2 \tag{12}$$

where $k_{LP}$ will be a constant also.

With a similar approach the pressure drop coefficient $\xi_{HP}$ of Eq. 2 for the high pressure loop can be expressed by

$$\xi_{HP} = k_{HP} \left( \frac{\dot{m}_C \sqrt{\theta_1}}{\delta_2} \right)^2 (1 - \mu)^2 \tag{13}$$

if it is assumed that the leakage factor $\mu$ of Eq. 1 is entirely due to flow through the bypass control valve.

The measured pressure drop coefficients $\xi_{LP}$ and $\xi_{HP}$ of the ML-1 loop are plotted in Fig. 6. With these data the coefficients $k_{LP}$ and $k_{HP}$ of Eqs. 12 and 13 were determined, and are shown in Fig. 6 also. It can be noted that $k_{LP}$ is very nearly constant, whereas $k_{HP}$ decreases somewhat with increasing referred flow rates. This condition is probably due to the widely changing temperatures in the high pressure loop. The results of Fig. 6 will be used for the subsequent system analysis.

## GRAPHICAL SOLUTION OF MATCHING PROBLEM

Eq. 1 will be expressed with the referred flow rates of the turbine and the compressor, as used in Eqs. 5 and 7.

$$\frac{\dot{m}_T \sqrt{\theta_3}}{\delta_3} = \frac{\dot{m}_C \sqrt{\theta_1}}{\delta_2} \frac{p_2}{p_3} (1 - \mu) \sqrt{\frac{T_3}{T_1}}$$

With Eq. 2

$$\frac{\dot{m}_T \sqrt{\theta_3}}{\delta_3} = \frac{\dot{m}_C \sqrt{\theta_1}}{\delta_2} \frac{1 - \mu}{1 - \xi_{HP}} \sqrt{\frac{T_3}{T_1}} \tag{14}$$

Further, from Eq. 4

$$r_T = r_C \frac{1 - \xi_{HP}}{1 + \xi_{LP}} \tag{15}$$

By taking the logarithms of the terms of Eqs. 14 and 15, and by considering the values thus obtained from Eq. 14 as vector components in the directions of the unit vectors $\bar{i}$, those from Eq. 15 as vector components in the directions of the unit vectors $\bar{j}$ of Figs. 2 and 3, and performing a vector addition, there is

$$\bar{i}\left[\log\left(\frac{\dot{m}_T\sqrt{\theta_3}}{\delta_3}\right) + \bar{j}\log r_T = \bar{i}\left[\log\left(\frac{\dot{m}_C\sqrt{\theta_1}}{\delta_2}\right)\right] + \bar{j}\log r_C\right.$$

$$\left. + \bar{i}\left[\log\left(\frac{1-\mu}{1-\xi_{HP}}\right)\frac{T_3}{T_1}\right)\right] + \bar{j}\log\left(\frac{1-\xi_{HP}}{1+\xi_{LP}}\right) \qquad (16)$$

With this procedure it has been possible to separate completely the turbine performance data (two terms on the left-hand side of Eq. 16) and the compressor performance data (first two terms on the right-hand side of Eq. 16) from those parameters which are affected only by the conditions in the system that connects the turbomachines, or by the temperatures at which heat is added to or dissipated from the cycle. The last two terms of Eq. 16 will therefore be called the system transfer vector $\bar{S}$, whereas the two terms on the left-hand side are denoted by $\bar{T}$, and the first two terms on the right-hand side by $\bar{C}$. Then, the vector relation

$$\bar{T} = \bar{C} + \bar{S} \qquad (17)$$

satisfies the matching condition of the turbine and the compressor for a particular loop. Since an arbitrary constant vector can be added to $\bar{T}$ and $\bar{C}$ without invalidating Eq. 17, the system transfer vector $\bar{S}$ indicates simply how points with the same coordinates in the turbine and compressor maps of Figs. 2 and 3 must be displaced in $\bar{i}$ and $\bar{j}$ directions to account for the systems characteristics in the matching solution. Possible solutions are then obtained for $N_T = N_C$, or

$$\frac{N_T}{\sqrt{\theta_3}} = \frac{N_C}{\sqrt{\theta_1}}\sqrt{\frac{T_1}{T_3}} \qquad (18)$$

where the ratio $T_3/T_1$ is again depending only on the imposed temperature limits, and not on the performance maps. Hence, if performance maps of the turbine and the compressor that are drawn on transparent paper are displaced in accordance with the vector $\bar{S}$, the possible operating points of the machines can be found at the intersection of the characteristics that satisfy Eq. 18.

From Eq. 16

$$\bar{S} = \bar{i}\left[\frac{1}{2}\log\left(\frac{T_3}{T_1}\right) + \log(1-\mu)\right] - \bar{j}\left[\log(1+\xi_{LP})\right]$$

$$+ (\bar{j} - \bar{i})\left[\log(1-\xi_{HP})\right] \qquad (19)$$

Fig. 7 shows a diagram for the determination of the vector $\bar{S}$. With the unit vectors $\bar{i}$ and $\bar{j}$ in the same directions as the corresponding vectors in Figs. 2 and 3, the vectors $\bar{S}$ obtained from Fig. 7 have their origins at a particular station, say $X_T$, in the turbine flow diagram and their termini at the station $X_C$ in the compressor flow diagram which has the same coordinates as $X_T$ (see Fig. 8).

From Fig. 7 it is evident how the different system parameters influence the vector $\bar{S}$. For instance, leakage or bypass flow has the same effect as a reduction in turbine inlet temperature. If $T_3/T_1$ is the actual ratio of turbine and compressor inlet temperatures, a certain bypass flow, expressed by the factor $\mu$, is effectively reducing this ratio to

$$\frac{T_3}{T_1}^* = \frac{T_3}{T_1} (1 - \mu)^2$$

Hence, for $T_3 = 1200^oF$ and $T_1 = 118^oF$ a leakage flow rate of 5% of $\dot{m}_C$ has the same effect as a reduction of the turbine inlet temperature from $1200^oF$ to about $1040^oF$. This example shows that output control by means of bypass flow is very effective, but it shows also the detrimental effect of internal leakage flows from the high pressure to the low pressure side of the loop.

## EXAMPLE

In Fig. 8 are shown the compressor and turbine flow maps of Figs. 2 and 3 displaced in accordance with the system transfer vector $\bar{S}$ from a station $X_T$ to a station $X_C$, which have the same coordinates in the respective maps. This shift of the coordinates establishes the graphical solution of Eq. 17. Since the pressure drop coefficients $\xi_{HP}$ and $\xi_{LP}$ depend on the flow rate and pressure ratio to be determined, the actual vector $\bar{S}$ must be obtained with a method of successive approximations. The pressure drop coefficients were determined with Eqs. 12 and 13, using the average values $k_{LP} = 0.0036$ and $k_{HP} = 0.0525$ from Fig. 6. The matching is carried out for $T_3 = 1200^oF$, $T_1 = 118^oF$, and a bypass flow of 3% of the compressor flow rate, at the nominal design speeds of the TC sets. Table 1 shows the match point conditions obtained from the points of intersection of corresponding characteristics in Fig. 8.

Table 1 Match Point Solutions from Fig. 8

| TC Set | A | B |
|---|---|---|
| $\frac{\dot{m}_C\sqrt{\theta_1}}{\delta_2}$ (lbm/sec) | 1.362 | 1.375 |
| $r_C = p_2/p_1$ | 2.725 | 2.285 |
| $\frac{\dot{m}_T\sqrt{\theta_3}}{\delta_3}$ (lbm/sec) | 2.460 | 2.480 |
| $r_T = p_3/p_4$ | 2.38 | 2.00 |
| $\xi_{LP}$ | 0.049 | 0.036 |
| $\xi_{HP}$ | 0.090 | 0.091 |

With these data it is possible to determine the shaft powers of the TC sets from Figs. 4 and 5, where the match points of Table 1 are denoted by $M_A$ and $M_B$.

The power of the TC sets will be calculated for a compressor inlet pressure $p_1 = 117.6$ psia or $\delta_1 = 8$, since higher pressures $p_1$ produce excessive stresses in the reactor vessel. The results are listed in Table 2.

Table 2. Power of TC Sets for Match Point Solutions of Fig. 8.

| | | |
|---|---|---|
| $\frac{KW_C}{\delta_1\sqrt{\theta_1}}$ (KW), (Fig.4) | 218.0 | 149.6 |
| $\frac{KW_T}{\delta_3\sqrt{\theta_3}}$ (KW), (Fig.5) | 60.2 | 48.0 |
| $\delta_3 = (1 - \varepsilon_{HP})\ \delta_2 = (1 - \varepsilon_{HP})\ \delta_1 \frac{P_2}{P_1}$ | 21.80 | 18.28 |
| $KW_T$ (KW) | 2135 | 1429 |
| $KW_C$ (KW) | 1842 | 1264 |
| $KW_S = KW_T - KW_C$ (KW) | 293 | 165 |

## DISCUSSION

The specifications for the TC sets called for a shaft power of about 480 KW at the design point. The reasons for the power deficiency of the sets become evident from Figs. 2 and 3 where the match point solutions of Table 1 are marked by $M_A$ and $M_B$ for the TC sets A and B.

At the specified design point the referred turbine flow rate should be 2.33 lbm/sec. Fig. 3 and Table 1 show that the actual flow rates of the TC sets A and B exceed this value by about 5½% and 6½%, respectively, at the match points. The compressor of TC set A is therefore forced to operate at an efficiency of about 80% whereas it could have about 84% if the flow rate were lower. Although the efficiency of the compressor of TC set B is generally lower than the design estimates, a reduced turbine flow rate would make it possible to operate the compressor at an

efficiency of about 78.5% instead of at about 76.5% at the match point. The increased flow rates also cause higher pressure drops on the high pressure side of the loop since $\zeta_{HP}$ is now about 9% instead of about 6% in accordance with the design point data.

The turbines of the TC sets have flow areas of about 10 sq.in. at the discharge of the rows of blades, where the throat widths of the flow channels between neighboring blades are between 0.15 and 0.20 in.. If the blade profiles have machining tolerances of $\pm$ 0.002 in., changes in flow area of between 2 and 4% are possible within the specified tolerances. The writer is also of the opinion that the usual calculating methods for turbines must not be applied to small turbines without giving special attention to the dimensioning of the flow areas. It is common practice to use the same loss coefficients for the efficiency and the flow area calculations. However, since the flow rates will be depending on the flow conditions at the throat of the blades, rather than on the conditions after them, it is necessary to apply smaller losses for the area calculations. If this is not done the flow areas will be larger than necessary. To investigate these conditions a computer program was established [1]*, which uses the blading losses of [2]. Only the so-called profile losses are applied to the flow area calculations by establishing an equivalent displacement thickness of the boundary layers at the throat areas of the blades. This program, which also takes account of after-expansions if the flow is chocked at the discharge of a blade row by applying the relations of [3], iterates accurately the flow conditions after each row of blades, and produces complete performance maps for different speeds and arbitrary fluids. Although at present restricted to two-stage turbines, designs with an arbitrary number of stages can be investigated with slight modifications of the program.

Another computer program [4] was set up to investigate means for improving the performance of the axial compressor of TC set B, and of

*Numbers in brackets designate References at end of paper.

shifting its characteristics to higher flow rates by increasing the stagger angles of the guide vanes. The program is based on the cascade data of [5] and takes account of the tip clearance, end, and secondary losses with the relations of [6]. The losses in the entrance and discharge passages of the compressor are considered also, and the program calculates the performance of each row of blades, and iterates exactly the flow conditions after each row. The deterioration of the velocity profiles toward the compressor discharge is taken into account by introducing blockage factors due to wall boundary layers, and work-done factors because of pointed velocity profiles. The two last-mentioned fa factors were obtained for the machine at hand by applying a variational process until the calculated performance matched the available test results. Additional work in this direction is presently carried out at the Propulsion Laboratory of the United States Naval Postgraduate School, where tests are being made with a completely instrumented twelve-stage axial compressor.

In the following it will be demonstrated what improvements of the TC sets A and B are possible with the existing compressors, by simply reducing the turbine flow rates to levels where the compressors can operate near their maximum efficiency. The chosen operating points are denoted by $0_A$ and $0_B$ in Fig. 2. The modified turbines are supposed to have about the same efficiency as the original designs, namely, 81% for TC set A and 80% for TC set B. The results are shown in Table 3 for $\delta_1 = 8$.

Hence by simply reducing the turbine flow areas, the shaft powers can be increased by about 25% and 65% for TC sets A and B, respectively. If at the same time the turbine efficiency of both sets could be improved to 85% the shaft powers would be 455 KW and 383 KW, respectively, for sets A and B.

These results clearly show that the proper matching of turbines and compressors in closed-cycle gas turbine plants is of utmost importance. Even machines with high efficiencies will not produce the required plant power if a mismatch prevents them to operate at the optimum efficiency.

Table 3 Operating Performance of TC Sets for Turbines with Reduced Flow Areas

| TC Set | A | B |
|---|---|---|
| $\frac{\dot{m}_C \sqrt{\theta_1}}{\delta_2}$ (lbm/sec) | 1.15 | 1.15 |
| $r_C = p_2/p_1$ | 2.900 | 2.665 |
| $\xi_{HP}$ | 0.065 | 0.065 |
| $\xi_{LP}$ | 0.040 | 0.038 |
| $r_T = p_3/p_4$ (Eq. 4) | 2.605 | 2.410 |
| $KW_C$ (KW) | 1671 | 1439 |
| $KW_T$ (KW) | 2036 | 1714 |
| $KW_S = KW_T - KW_C$ | 365 | 275 |

ACKNOWLEDGEMENTS

The writer thanks Aerojet-General Nucleonics, the Atomic Energy Commission, and the Department of the Army of the United States, for granting permission to publish this paper which originated in 1961 in connection with work performed under Contract No. DA-44-192 Eng.-8, and submitted as report AN-ENGR-35 in a somewhat different form. Thanks are also due to my friend and colleague, Dr. T. H. Gawain, Professor, USNAVPGSCOL, who drew my attention to the possibility of solving matching problems with this graphical method.

# BIBLIOGRAPHY


1. "Method for Evaluation of Performance of Two-Stage Turbines", M. H. Vavra, Report AN-AGCR-217, Aerojet-General Nucleonics, May 1962.

2. "A Method of Performance Estimation for Axial-Flow Turbines", D. G. Ainley, and G. C. R. Mathieson, Aeronautical Research Council of Great Britain, R. & M. No. 2974, December 1951.

3. "Thermische Turbomaschinen", W. Traupel, Springer-Verlag, Berlin, 2nd. ed., 1962, pp. 220-226.

4. "Analysis of Performance of Axial-Flow Compressor for ML-1", M. H. Vavra, Report AGN-VA #26, Aerojet-General Nucleonics, November 1963.

5. "Aerodynamic Design of Axial-Flow Compressors", Vol. II, NACA Research Memorandum RM E 56 BO3a, August, 1956.

6. "Aerothermodynamics and Flow in Turbomachines", M. H. Vavra, Wiley and Sons, Inc., N. Y. 1960, p. 380.

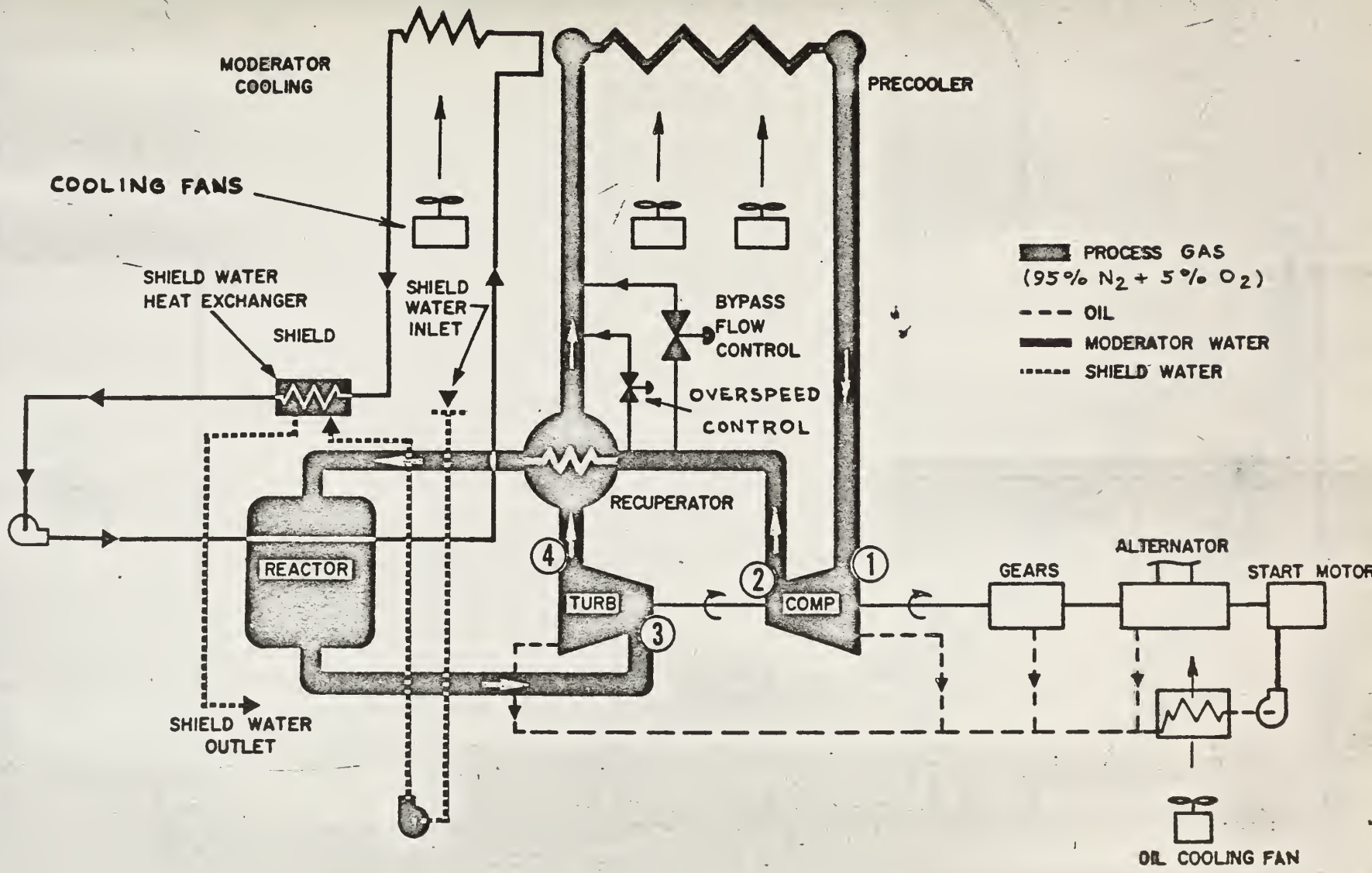


Flow Diagram and Schematic of ML-1 Closed-Cycle Nuclear Gas Turbine Plant of Aerojet-General Nucleonics.

M.H. VAVRA FIG. 1

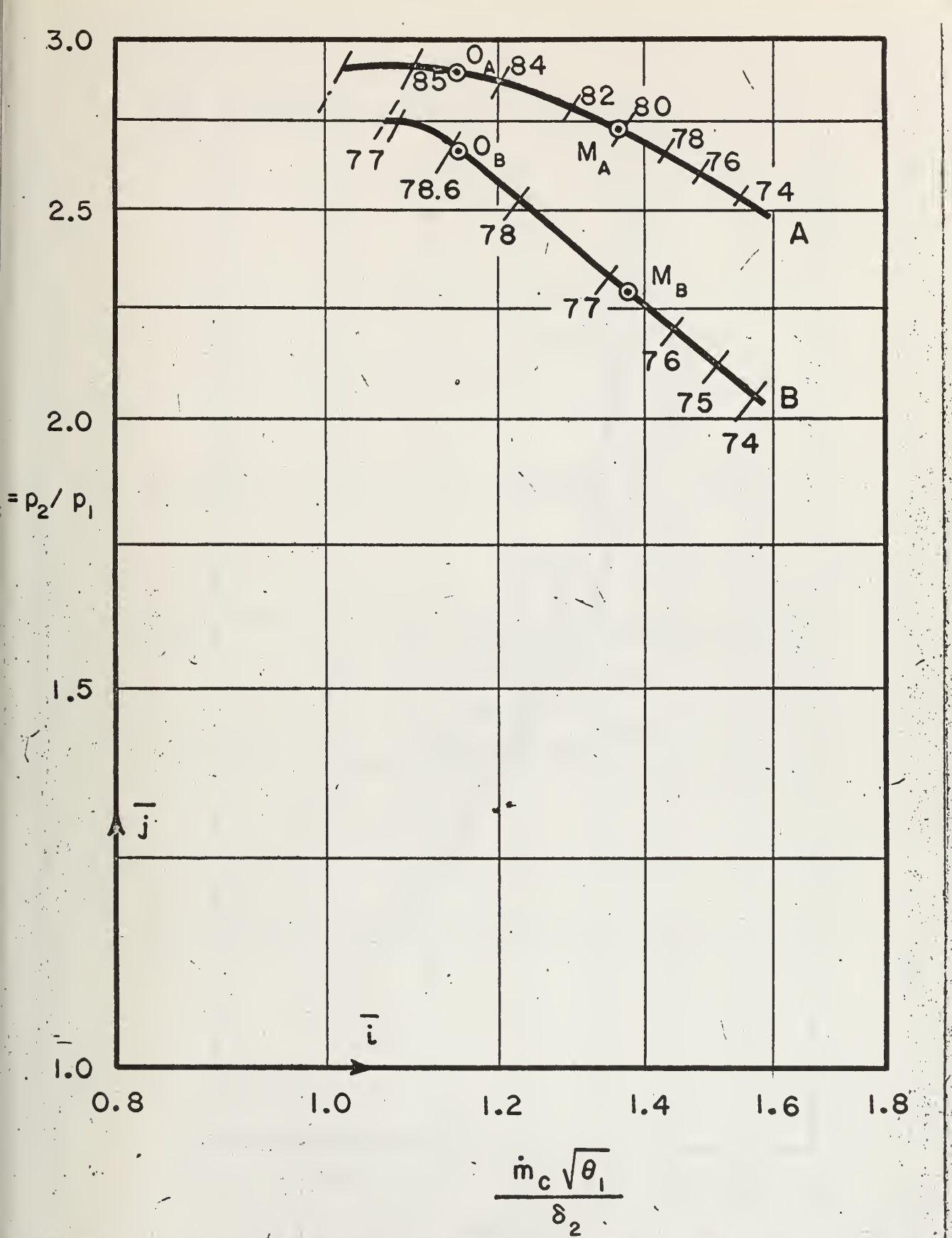


VAVRA FIG. 2 Referred Flow Rates of Compressors of Turbocompressor Sets as Function of Pressure Ratio $p_2/p_1$.

Curve A is for Two-Stage Radial Compressor at a referred Speed $N_C/\sqrt{\theta_1}$ = 17,170 rpm

Curve B is for 11-Stage Axial Compressor at a referred Speed $N_C/\sqrt{\theta_1}$ = 20,620 rpm

$\dot{m}_C$ = Mass Flow Rate (lbm/sec); $\theta_1 = T_1/T_{ATM}$; $\delta_2 = p_2/p_{ATM}$; M = Match points; O = Optimum Operating Points. (The numbers adjacent to the curves represent the compressor efficiencies in percent). ($\bar{i}$ and $\bar{j}$ represent unit vectors in the directions of the coordinates).

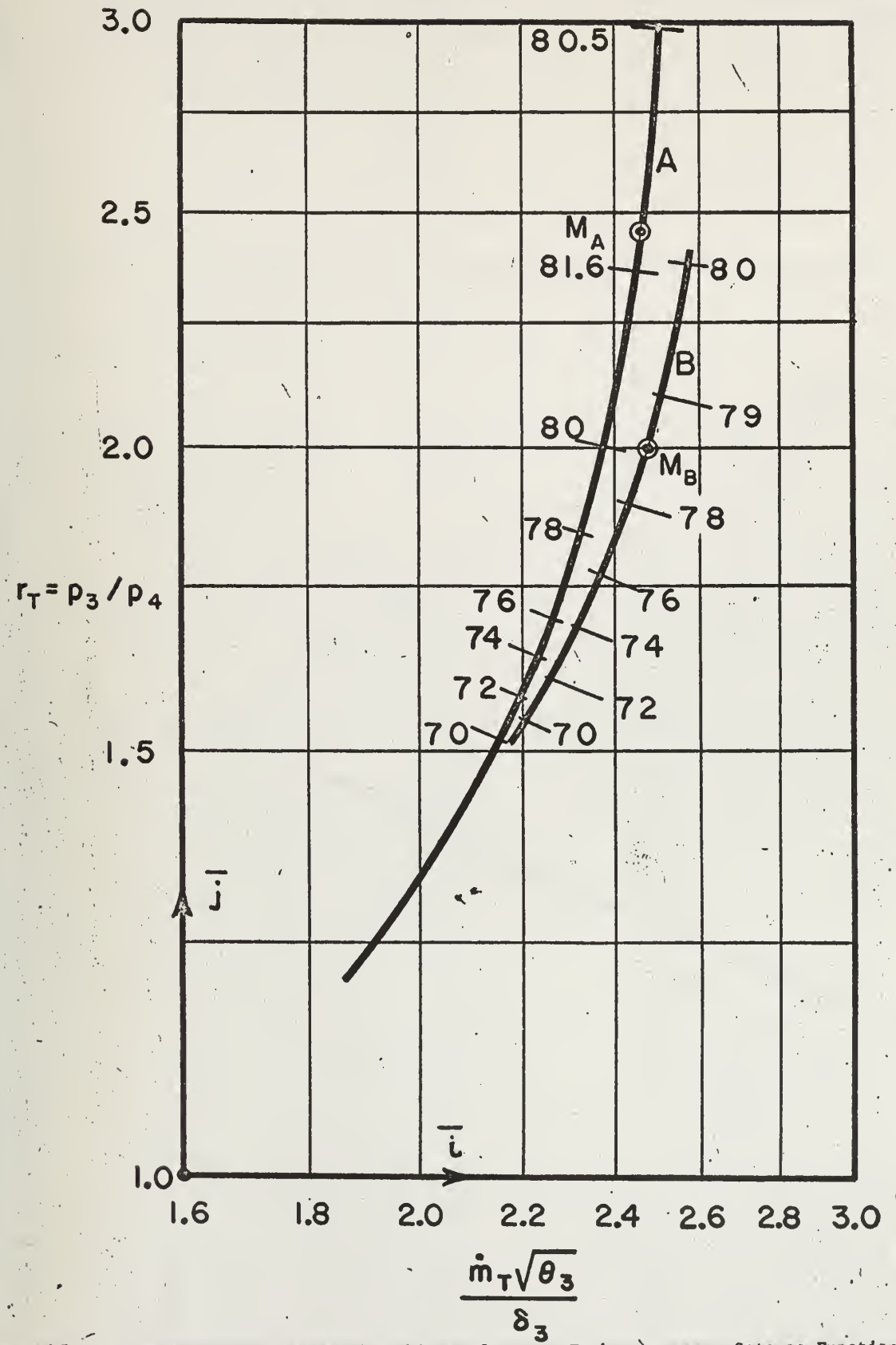


VAVRA FIG. 3 Referred Flow Rates of Turbines of Turbocompressor Sets as Function of Pressure Ratio $p_3/p_4$.
Curve A is for Turbine of Set A at a referred Speed $N_T/\sqrt{\theta_3}$ = 10,130 rpm
Curve B is for Turbine of Set B at a referred Speed $N_T/\sqrt{\theta_3}$ = 12,160 rpm
$\dot{m}_T$ = Mass Flow Rate (lbm/sec); $\theta_3 = T_3/T_{ATM}$; $\delta_3 = P_3/P_{ATM}$; M = Match Points
(The numbers adjacent to the curves represent the turbine efficiencies in percent).

Vavra Fig.4

Referred Power of Compressors of Turbocompressor Sets.
Curve A is for Compressor of Set A at a referred Speed $N_C/\sqrt{\theta_1}$ = 17,170 rpm
Curve B is for Compressor of Set B at a referred Speed $N_C/\sqrt{\theta_1}$ = 20,620 rpm

$KW_C$ = Compressor Power (KW)
M = Match Points
O = Optimum Operating Points

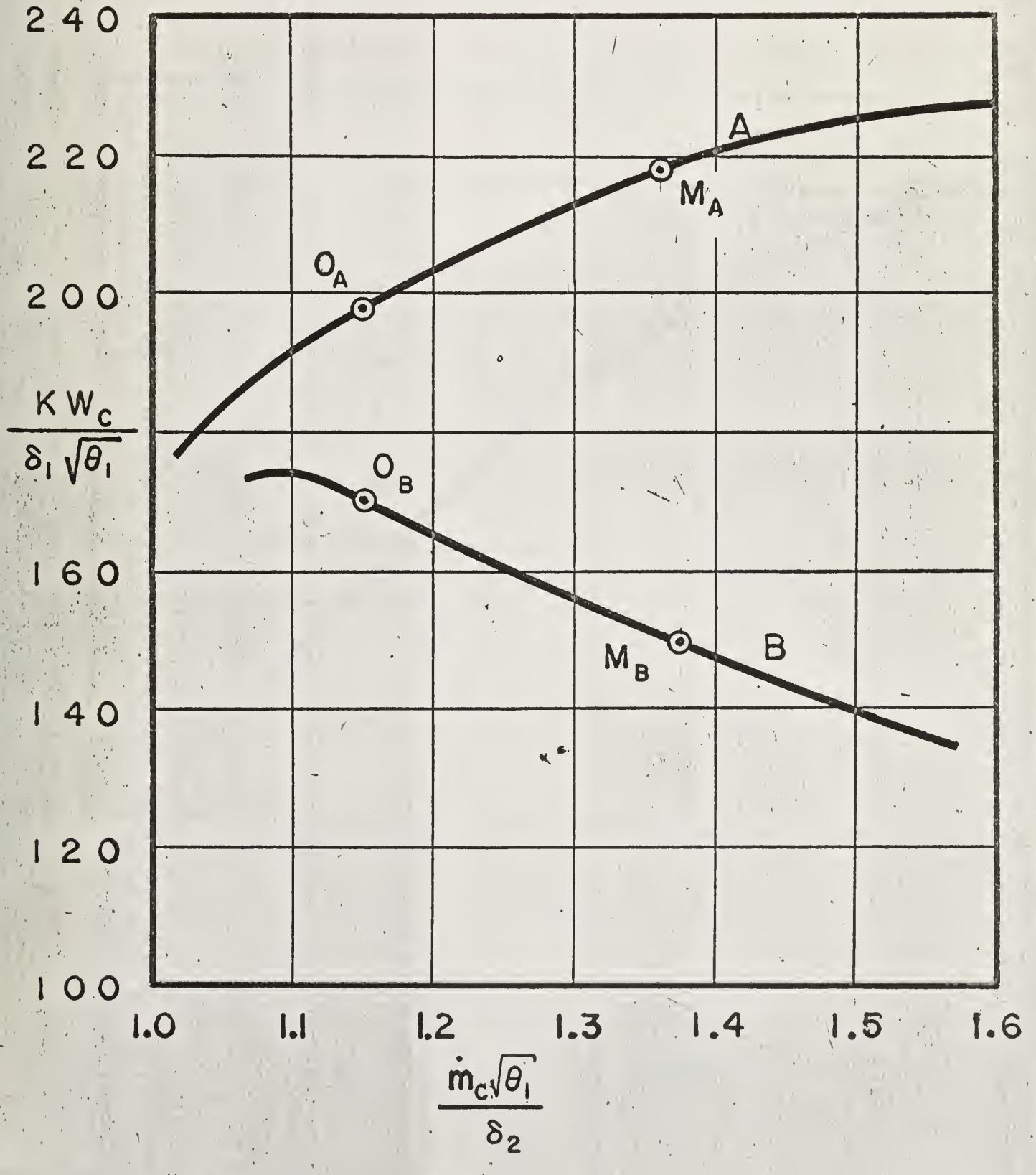

M. H. VAVRA Fig. 5 Referred Power of Turbines of Turbocompressor Sets.

Curve A is for Turbine of Set A at a referred Speed
$N_T/\sqrt{\theta_3}$ = 10,130 rpm

Curve B is for Turbine of Set B at a referred Speed
$N_T/\sqrt{\theta_3}$ = 12,160 rpm

$KW_T$ = Turbine Power (KW)

M = Match Points

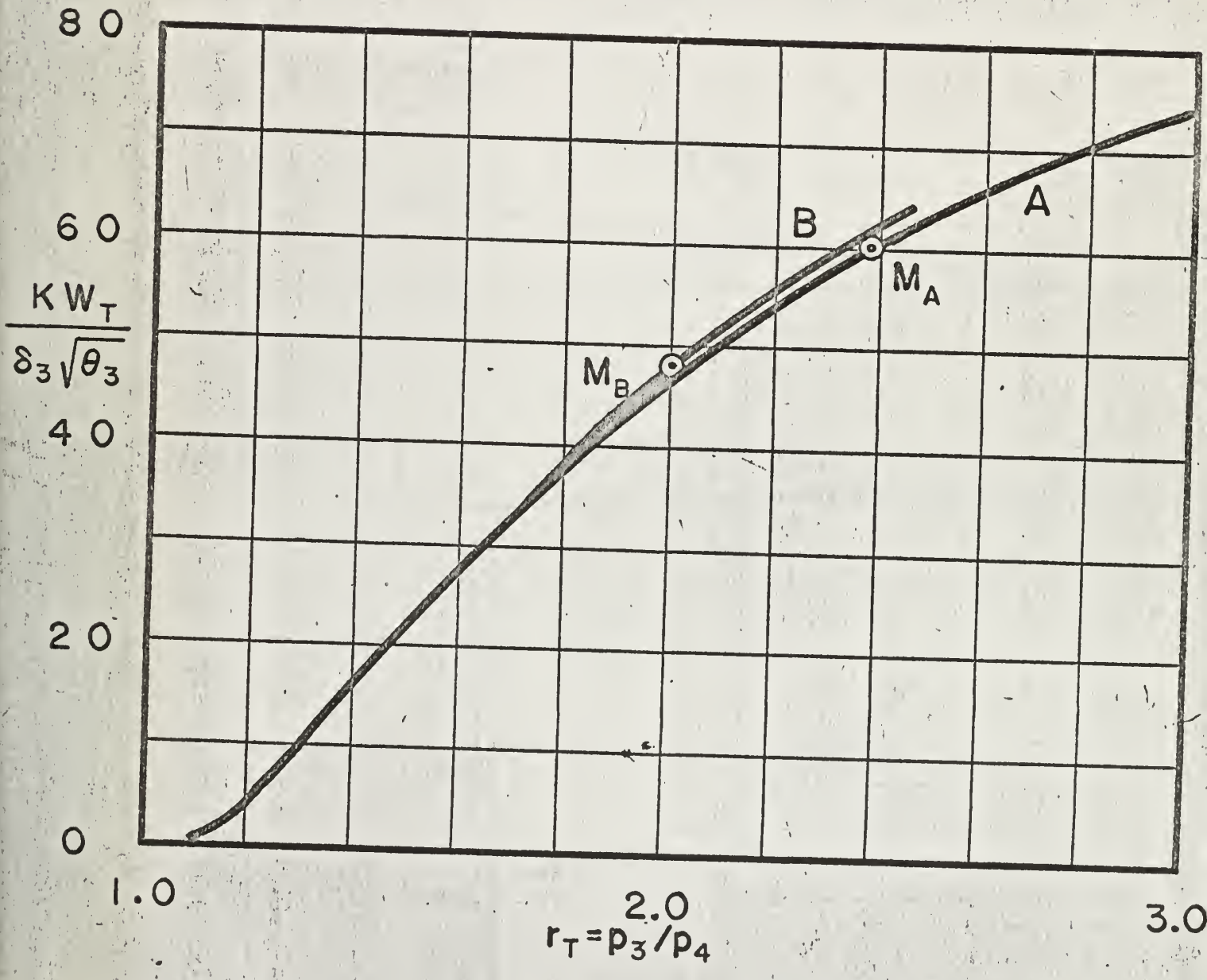




vra, Fig. 5

Pressure Drops in System of ML-1 Plant.

$$\xi_{HP} = \frac{p_2 - p_3}{p_2}$$

$k_{HP}$ calculated from Eq. 13

$$\xi_{LP} = \frac{p_4 - p_1}{p_1}$$

$k_{LP}$ calculated from Eq. 12

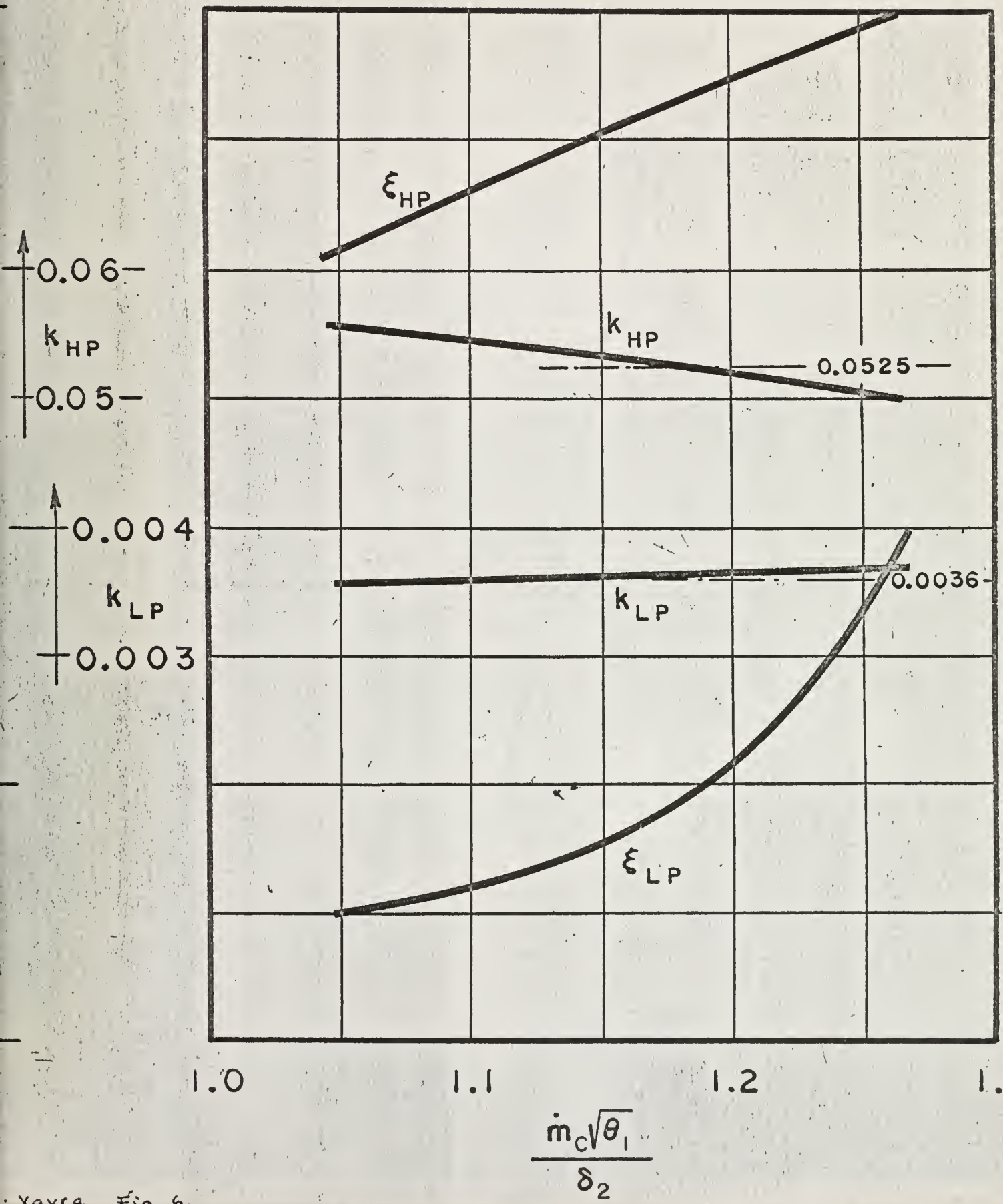


Yavra Fig. 6

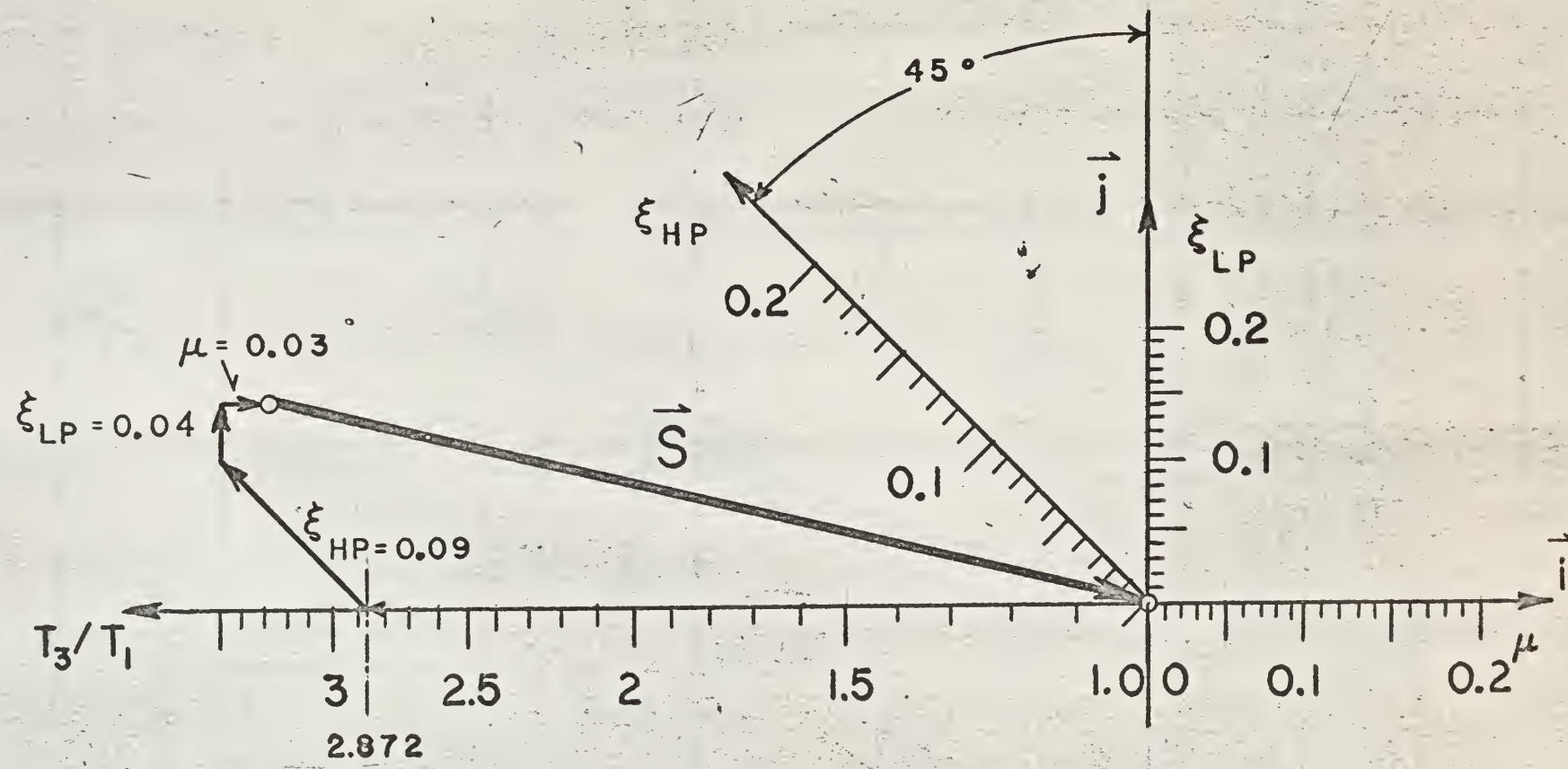


M. H. Vavra Fig. 7 Diagram for the Determination of the System Transfer Vector S . Values for Example: $T_3/T_1 = 2.872$

$\xi_{LP} = 0.04$ $\mu = 0.03$ $\xi_{HP} = 0.09$

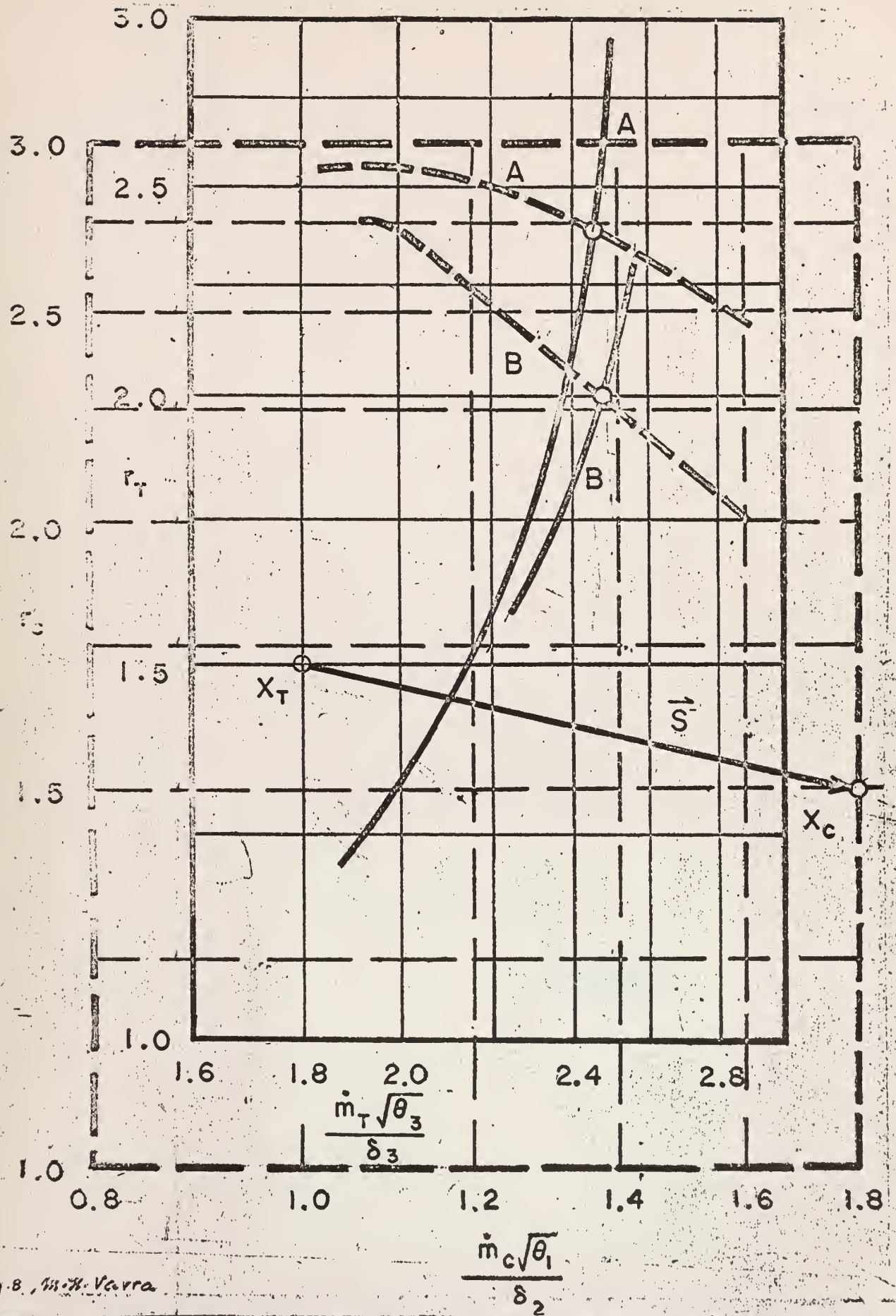


Fig. 8, W. H. Vavra

Graphical Matching Solution. (The diagram shown with dashed lines is identical with Fig. 2, and superimposed on Fig. 3 (shown with solid lines). The displacement of the figures is given by the System Transfer Vector S of Fig. 7, to obtain the matching solutions for the system).